0026-895X/89/050720-09$02.00/0

MOLECULAR PHARMACOLOGY, 35:720-728

Molecular Modelling of DNA-Antitumour Drug Intercalation Interactions: Correlation of Structural and Energetic Features with Biological Properties for a Series of Phenylquinoline-8-carboxamide Compounds

R. MCKENNA, A. J. BEVERIDGE, T. C. JENKINS, S. NEIDLE, and W. A. DENNY

Cancer Research Campaign Biomolecular Structure Unit, The Institute of Cancer Research, Sutton, Surrey SM2 5NG, United Kingdom (R.M., A.J.B., T.C.J., S.N.) and Cancer Research Laboratory, University of Auckland Medical School, Auckland, New Zealand (W.A.D.)

Received October 11, 1988; Accepted January 17, 1989

SUMMARY

The crystal structure of the experimental antitumour compound *N*-(2-dimethylaminoethyl)-2-phenylquinoline-8-carboxamide has been determined. The geometry and conformation have been used as starting points for molecular modelling of the intercalative interactions with DNA shown by the parent compound and analogues with the phenyl ring located at alternative positions on the quinoline chromophore. A molecular mechanics force field program was used for energy minimization and calculation of intermolecular (enthalphic) binding energies. The parent quinoline-8-carboxamide and derivatives with a phenyl substituent at the 4- or 5-position were judged to be poor intercalators in both structural and energetic terms. By contrast, the 2-, 3-, and 6-phenyl derivatives all had high calculated binding energies with the phenyl groups involved in stacking with DNA base pairs. The order of energies calculated for this series of compounds has been found to correlate well with both the order of experimentally derived free energies and with the *in vitro* cytotoxic activity.

A number of studies (1–4) of the anticancer drug amsacrine **1**, a 9-aminoacridine derivative, have extensively explored the relationships between its cytotoxic and antitumour activities and the DNA-intercalating ability of the tricyclic acridine system. In general, for the many analogues of this compound that have been synthesized and examined, it has been found that DNA intercalation is a necessary, although by itself insufficient, property in order for high *in vivo* and *in vitro* activity to be shown. Thus, analogues with reduced levels of DNA binding, such as 1-methyl-amsacrine [which has a markedly nonplanar chromophore (5)], have much lower cytotoxicity and no antitumour activity. More recently, several new series of carboxamide-substituted acridines and 9-aminoacridines have been developed (6–9). These differ markedly in distribution properties, with acridine-4-carboxamides (e.g., **2**) having a neutral acridine chromophore at physiological pH whereas the 9-aminoacridine analogues (e.g., **3**) have pK_a values of approximately 8.3 for the acridine ring nitrogen atom and are, thus, essentially dicationic in solution at pH 7–7.4. The acridine-4-carboxamides have significant activity against murine solid tumour models (8).

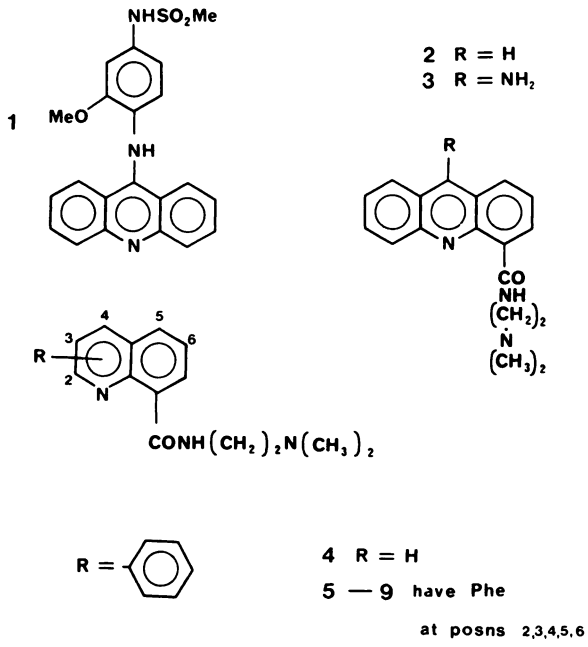

In an effort to develop compounds that have lower DNA affinities than those in the tricyclic series yet retain intercalative ability, a series of substituted quinolines, **4–9**, were evaluated that have a carboxamide side-chain at the 8-position and a phenyl group at differing sites on the quinoline chromophore (10). The reduction in the size of the potential intercalating chromophore to a bicyclic system was rationalized on the basis

We are grateful to the Cancer Research Campaign for continuing support and to the Institute of Cancer Research for a research studentship (to R.M.). W.A.D. thanks the Auckland Division of the Cancer Society of New Zealand for support.

of possible improved distribution properties as well as reduced generalized binding to cellular macromolecules. Five isomeric phenylquinoline-8-carboxamides, **5–9**, together with the unsubstituted parent compound, quinoline-8-carboxamide **4**, were examined in this study (10). It was found that the position of phenyl ring attachment on the chromophore was critical for the ability of a derivative to effectively intercalate into DNA. This property was also directly related to *in vitro* and *in vivo* biological activities in the series, with the 2-phenyl derivative **5** being outstanding in all respects.

The present study uses molecular modelling techniques to rationalize the DNA-binding behavior of this series of phenylquinoline compounds in terms of detailed plausible structural models and, thus, to develop structure-activity relationships. X-ray crystallography has been used to define the geometry and conformation of the 2-phenyl compound **5**.

Materials and Methods

Crystal structure of *N*-(2-dimethylaminoethyl)-2-phenylquinoline-8-carboxamide 5. Bright yellow crystals of **5**, as the dihydrochloride salt, were grown from ethanol/water. A crystal of irregular shape and dimensions roughly 0.5 × 0.5 × 0.4 mm was used for all structural work. Table 1 gives a summary of the crystallographic data. Preliminary Weissenberg photographs showed no systematic absences. Cell dimensions were obtained from least squares refinement of 25θ values ($10° < \theta < 25°$) measured on an Enraf-Nonius CAD-4 diffractometer; Ni-filtered CuK_α radiation was used. Intensity data were collected with an ω–2θ scan technique and a maximum scan time of 100 sec/reflection for $1.5° \leq \theta \leq 65.0°$ and $0 \leq h \leq 11$, $-15 \leq k \leq 15$, $-22 \leq l \leq 22$. A total of 7631 reflections were measured, of which 4366 were judged to be significant with $I \geq 3\sigma(I)$ for 7094 unique reflections. A periodic check on three standard reflections during the data collection did not indicate any significant radiation decay. The structure was solved by direct methods using the MULTAN82 program (11), as implemented in the SDP crystallographic program system (12), and an empirical absorption correction was applied (13). Scattering factors were taken from *International Tables for X-Ray Crystallography (1974)*. The most consistent *E*-map revealed the position of four chlorine atoms (showing the presence of two independent molecules, referred to as A and B, within the asymmetric unit) and two fused six-membered rings. The remaining atoms were found in difference Fourier syntheses. Refinement was carried out by full matrix, least squares, techniques with all nonhydrogen atoms being assigned anisotropic temperature factors. The positions of the majority of the hydrogen atoms, including those on the protonated nitrogen atoms, were determined from difference Fourier maps. The positions of the few remaining ones were generated by standard geometric considerations, except for the hydrogens of the water molecules, which were not located. All hydrogen atoms were assigned a fixed isotropic temperature factor of 5.0 Å^2, and some also had their positional parameters fixed. A non-Poisson distribution weighting scheme of the type $w = [\sigma^2(F) + (PF)^2]^{-1}$ was used, where *P* was given a value of 0.04. Refinement converged with a final *R* of 0.046 and R_w of 0.058. The final difference Fourier map showed some residual density with <0.91 *e* Å^{-3}; although this is high, the top 10 ranking peaks were close to the oxygen atoms of the water molecules but could not be unequivocally assigned as their attached hydrogen atoms. These features are most probably due to thermal motion of the water molecules in the crystal lattice.

TABLE 1

Crystal data for *N*-(2-Dimethylaminoethyl)-2-phenylquinoline-8-carboxamide (dihydrochloride dihydrate)

$C_{20}H_{23}N_3OCl_2 \cdot 2H_2O$
M_r = 414.36, triclinic, space group $P\bar{1}$, cell dimensions a = 9.490 (1), b = 12.833 (2), c = 19.266 (5) Å, α = 91.98 (2)°, β = 90.21 (1)°, γ = 108.05 (1)°, V = 2229.2 Å^3, Z = 4, D_α = 1.235 Mg m^{-3}, λ (CuK_α) = 1.54178 Å, μ = 2.8297 mm^{-1}, $F(000)$ = 876, T = 298K.
Final R = 0.046 for 4366 observed reflections with $I \geq 3\sigma(I)$.

Molecular Modelling. The structure of molecule A of *N*-(2-dimethylaminoethyl)-2-phenylquinoline-8-carboxamide **5** from the crystal structure analysis was used as a starting point. This was an arbitrary choice, because bond lengths and angles were not significantly different in the two independent molecules. Because the pK_a of the chromophore for all six compounds is <3.2 (10), the hydrogen atom on the protonated site at the N1 atom was removed in the modelling, in accord with biological conditions being between pH 7 and 7.4. This gives rise to the possibility of a hydrogen bond between N1 and the N18 hydrogen atom of the carboxamide, which was achieved by a change of the C9-C8-C17-N18 torsion angle by 180°. A similar situation has been described for *N*-(2-dimethylaminoethyl)- and *N*-(2-dimethylaminobutyl)-9-aminoacridine-4-carboxamides (14). The structures of the other five compounds were generated using the basic quinoline-8-carboxamide obtained from the crystal structure of **5**, by relocating the phenyl substituent at the 3-, 4-, 5-, or 6-position on the quinoline ring to produce structures for **6–9** and also by completely removing the phenyl group in the case of compound **4**. These building operations were performed on a Silicon Graphics IRIS workstation with the molecular modelling program GEMINI (15). Interactive computer graphics techniques were used to dock the compounds into a model of duplex DNA with an intercalation site. This model is of an alternating hexanucleotide sequence d(TACGTA) that has an intercalation site between the central CG base pairs (16). It has been derived from a decanucleotide complex constructed by means of least squares fitting of B-DNA residues to both ends of the d(CG) dinucleoside geometry found in its crystalline complex with proflavine (17), followed by energy minimization (18). The docking process was accompanied by alterations in the conformation of the ligand side-chain and phenyl ring in order to minimize bad intermolecular contacts. Positions of potential low energy were judged by maximum stacking of the quinoline ring with base pairs, together with minimal repulsive close contacts. Possible occupation of either the major or minor DNA groove by the carboxamide side-chain was considered for all six compounds. In the case of compounds **5** and **9**, the simultaneous positioning of both phenyl group and side-chain simultaneously in the same groove was examined. Drug conformations were also examined for intercalation models for **5** and **9** with the carboxamide side-chain rotated by 180° from its crystallographic orientation, so that the carbonyl oxygen atom was *trans* rather than *cis* to the ring nitrogen atom.

All intercalated complexes were subjected to molecular mechanics full geometry minimization. The force field used was of the form:

$$E(\text{total}) = E(\text{nonbonded}) + E(\text{electrostatic}) + E(\text{torsion}) + E(\text{angle}) + E(\text{bond})$$

The force field parameter set used for the DNA was an all-atom representation (18). Parameters for the ligand were in part as developed in previous studies from this laboratory (19) and are given in Table 2. Partial charges for the monocations of each of the compounds were obtained by CNDO/2 calculations. A distance-dependent dielectric constant of the form $\epsilon = 4r_{ij}$ (20) was used. Convergence was judged to have been achieved during the energy refinements after approximately 1000 cycles, when the root mean square value of the first derivative was less than 0.2 kcal mol^{-1} Å^{-1} in all cases. All calculations were performed on a VAX 11/750 computer using the EMPMDS program (21).

Results

Crystal Structure of Compound 5

In the crystallographic asymmetric unit, two independent molecules were found to be present, together with four chloride ions and four water molecules. The molecular structure of these

TABLE 2

Additional molecular mechanics force field parameters for the phenylquinoline-8-carboxamides

Dihedral twist barriers not explicitly included in Ref. 19 were set to values in accord with chemically and structurally equivalent atom types already existing in the parameter library. The equilibrium bond angle values are the mean of the crystallographic ones.

	Bond stretches	
No additional bond stretch parameters were needed.		
	Bond Angle Deformations	
	K_θ	Θ_o
	kcal mol^{-1} *rad*$^{-2}$	
CA-CB-CA	85	120.2°
NC-CB-CA	70	120.6°
NC-CA-CA	75	120.0°
CB-CA-C	85	120.1°
CT-N3-CT	50	110.1°

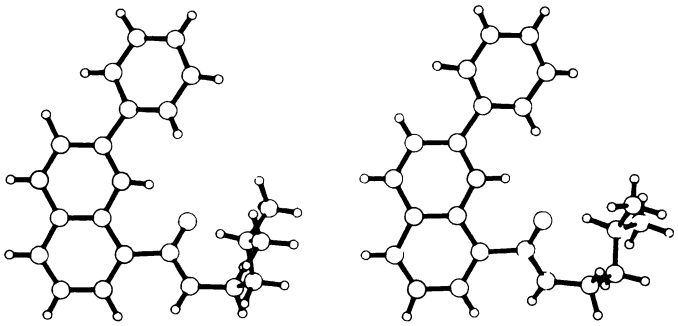

Fig. 1. Computer-drawn views of the molecular structures of the two independent molecules in the crystal structure of 2-phenylquinoline-8-carboxamide **5**. Molecule A is on the *left*.

two dihydrochloride salts are shown in Fig. 1, and atomic coordinates are given in Table 3. The two molecules A and B show no significant deviations in bond length and angle compared with each other or with quinoline-2-carboxamide (22). The phenyl and quinoline rings and the amide group are all planar in both A and B molecules. The phenyl ring and amide group are both twisted out of the plane of the quinoline ring, with closely similar torsion angles in A and B for the former (Table 4). The torsion angle around the C8-C17 bond differs by 10° for the two molecules. Table 4 shows that the side-chain conformations of the two molecules do not differ at any point by more than 8–10°. Intramolecular hydrogen bonding is apparent between the protonated ring nitrogen atom of each molecule and the amide oxygen atom, with H(N1) · · · 017 distances of 1.935(5) and 1.802(5) Å for molecules A and B, respectively. The chloride ions and water molecules in the crystal lattice create a network of electrostatic and hydrogen bond intermolecular interactions that involve the molecules of **5**.

Molecular Modelling of Drug-DNA Complexes

The results of the energy minimization calculations on the simulated complexes between the six quinoline compounds and the duplex intercalation site sequence d(TACGTA) (Fig. 2) are presented in Table 5. Sixteen models in total have been energy-refined, with each compound having its carboxamide side-chain in either the major or minor groove of the intercalated DNA. Each model was examined by interactive computer graphics procedures after refinement, and the results are presented below. Strand 1 is the d(TACGTA) molecule, reading 5′ to 3′,

TABLE 3

Non-hydrogen atom positional parameters and averaged thermal parameters, with ESDs in parenthesis, for compound 5

Atom designations A and B refer to the two independent molecules present within the asymmetric unit.

Atom	x	y	z	B_{eq}[a]
				Å^2
A				
N1A	1.874 (3)	1.0514 (2)	0.5524 (2)	3.27 (7)
C2A	1.2254 (5)	1.1589 (3)	0.5668 (2)	3.9 (1)
C3A	1.3404 (5)	1.2277 (3)	0.5276 (2)	4.8 (1)
C4A	1.4045 (5)	1.1837 (4)	0.4768 (2)	5.3 (1)
C5A	1.4325 (5)	1.0185 (4)	0.4129 (2)	5.6 (1)
C6A	1.3913 (5)	0.9085 (4)	0.4051 (2)	5.8 (1)
C7A	1.2776 (5)	0.8429 (4)	0.4442 (2)	4.6 (1)
C8A	1.2069 (4)	0.8877 (3)	0.4935 (2)	3.58 (9)
C9A	1.2511 (4)	1.0025 (3)	0.5027 (2)	3.36 (9)
C10A	1.3643 (5)	1.0703 (4)	0.4626 (2)	4.4 (1)
C11A	1.1463 (5)	1.1974 (3)	0.6219 (2)	4.0 (1)
C12A	1.0718 (6)	1.1279 (3)	0.6719 (2)	5.1 (1)
C13A	0.9971 (6)	1.1644 (4)	0.7237 (3)	6.6 (1)
C14A	0.9961 (6)	1.2718 (4)	0.7239 (3)	7.7 (1)
C15A	1.0671 (7)	1.3400 (4)	0.6736 (4)	8.5 (2)
C16A	1.1427 (6)	1.3034 (4)	0.6239 (3)	6.7 (1)
C17A	1.0794 (4)	0.8194 (3)	0.5339 (2)	3.37 (9)
O17A	0.9837 (3)	0.8584 (2)	0.5560 (1)	3.78 (6)
N18A	1.0738 (4)	0.7154 (3)	0.5429 (2)	4.03 (8)
C19A	0.9436 (5)	0.6367 (3)	0.5714 (3)	4.8 (1)
C20A	0.9615 (5)	0.6136 (3)	0.6461 (3)	5.1 (1)
N21A	0.9653 (4)	0.7049 (3)	0.6964 (2)	4.55 (9)
C22A	0.9931 (7)	0.6734 (4)	0.7682 (3)	7.1 (2)
C23A	0.8280 (6)	0.7381 (4)	0.6932 (3)	6.3 (1)
B				
N1B	0.6565 (3)	0.5626 (2)	0.9307 (2)	2.91 (7)
C2B	0.6786 (4)	0.6608 (3)	0.9048 (2)	3.03 (8)
C3B	0.7887 (5)	0.7496 (3)	0.9346 (2)	3.8 (1)
C4B	0.8725 (5)	0.7334 (3)	0.9887 (2)	4.2 (1)
C5B	0.9336 (5)	0.6063 (4)	1.0697 (2)	5.0 (1)
C6B	0.9031 (6)	0.5024 (4)	1.0919 (2)	5.7 (1)
C7B	0.7882 (5)	0.4165 (4)	1.0619 (2)	4.6 (1)
C8B	0.7043 (4)	0.4330 (3)	1.0083 (2)	3.26 (9)
C9B	0.7366 (4)	0.5407 (3)	0.9845 (2)	2.99 (8)
C10B	0.8503 (4)	0.6284 (3)	1.0146 (2)	3.53 (9)
C11B	0.5835 (4)	0.6688 (3)	0.8462 (2)	3.30 (9)
C12B	0.5151 (5)	0.5787 (3)	0.8030 (2)	3.8 (1)
C13B	0.4300 (5)	0.5892 (4)	0.7467 (2)	4.7 (1)
C14B	0.4113 (6)	0.6883 (4)	0.7342 (3)	5.7 (1)
C15B	0.4771 (6)	0.7773 (4)	0.7769 (3)	5.9 (1)
C16B	0.5636 (5)	0.7694 (3)	0.8326 (2)	4.8 (1)
C17B	0.5790 (5)	0.3428 (3)	0.9751 (2)	3.48 (9)
O17B	0.4830 (3)	0.3641 (2)	0.9399 (1)	3.70 (6)
N18B	0.5746 (4)	0.2397 (3)	0.9864 (2)	4.12 (8)
C19B	0.4524 (5)	0.1465 (3)	0.9581 (2)	4.7 (1)
C20B	0.4923 (5)	0.0977 (3)	0.8927 (2)	4.4 (1)
N21B	0.5178 (4)	0.1702 (3)	0.8329 (2)	4.55 (9)
C22B	0.5856 (7)	0.1204 (4)	0.7755 (2)	6.4 (2)
C23B	0.3837 (6)	0.1021 (4)	0.8069 (3)	6.9 (1)
Chloride ions and water molecules oxygens				
CL1	0.7499 (1)	0.39778 (8)	0.81943 (5)	3.92 (2)
CL2	1.2956 (1)	0.57370 (8)	0.54955 (6)	4.69 (3)
CL3	1.2325 (1)	0.91111 (8)	0.69777 (6)	4.02 (2)
CL4	0.8551 (2)	0.0420 (1)	0.89848 (7)	6.06 (3)
OW1	0.4143 (4)	0.4877 (3)	0.4119 (2)	5.88 (9)
OW2	0.7651 (4)	0.1309 (3)	0.0403 (2)	7.0 (1)
OW3	0.1014 (5)	0.9342 (4)	0.8490 (2)	9.1 (1)
OW4	0.3857 (7)	0.6599 (3)	0.3330 (2)	12.0 (2)

[a] The equivalent isotropic thermal parameter, for atoms refined anisotropically, is defined by the equation: $1.333(a^2B_{11} + b^2B_{22} + c^2B_{33} + bcB_{23}\cos\alpha + acB_{13}\cos\beta + abB_{12}\cos\gamma)$.

TABLE 4

Selected torsion angles found in the crystal structure of compound 5

Standard deviations average 0.5°.

Atom 1	Atom 2	Atom 3	Atom 4	Molecule A	Molecule B
C7	C8	C17	017	−151.4	−161.4
C7	C8	C17	N18	27.1	17.3
N1	C9	C8	C17	5.7	1.3
N1	C2	C11	C12	20.8	23.8
C8	C17	N18	C19	−170.0	−177.6
C17	N18	C19	C20	−102.9	−98.8
N18	C19	C20	N21	70.7	66.7
C19	C20	C21	C22	−176.5	−168.9
C19	C20	N21	C23	59.2	67.8
017	C17	N18	C19	8.5	1.2

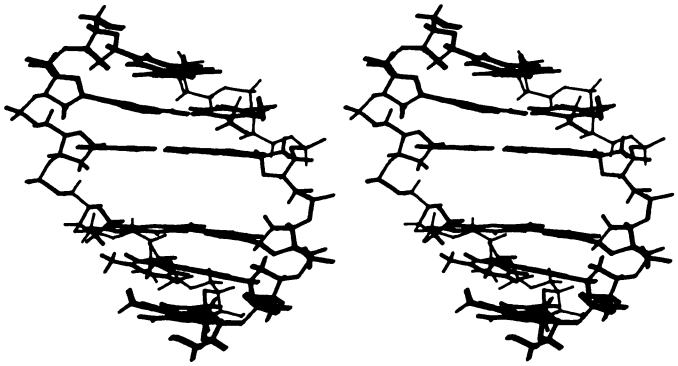

Fig. 2. Stereo view of the d(TACGTA) duplex with an intercalation site between the CG base pairs.

TABLE 5

Summary of energy minimization calculations

Energies are in kcal mol^{-1}, where $\Delta E = E_{complex} - (E_{drug} + E_{DNA})$.

Compound	Groove for side-chain	$\Delta E_{complex}$	E_{drug}	ΔE	Model Number
		kcal mol^{-1}			
4	Minor	−287.9	−0.2	−15.9	1
	Major	−285.1	−0.2	−13.1	2
5	Minor	−287.3	−0.6	−14.9	3
	Major	−288.1	−0.6	−15.7	4
5*	Minor	−294.0	−0.5	−21.6	5
	Major	−271.1	−0.6	1.2	6
6	Minor	−290.3	1.7	−20.2	7
	Major	−285.3	1.7	−15.2	8
7	Minor	−286.4	5.0	−19.4	9
	Major	−283.9	5.0	−17.1	10
8	Minor	−285.2	4.9	−18.3	11
	Major	−282.3	4.9	−15.4	12
9	Minor	−299.1	1.8	−29.2	13
	Major	−283.9	1.8	−13.9	14
9*	Minor	−282.0	1.8	−12.0	15
	Major	−265.2	1.8	4.8	16

* These compounds have their chromophore-carboxamide torsion angle around bond C8-C17 approximately at the crystallographically observed value. The calculated energy (E_{DNA}) for the intercalated hexamer duplex, without drug, was −271.8 kcal mol^{-1}.

that has the cytosine on the 5′ side of the intercalation site. Strand 2 is its complement.

Quinoline-8-carboxamide 4. The minor groove carboxamide model (Fig. 3) has its side-chain close to the strand 2 guanosine at the intercalation site, so that one terminal methyl group is in close contact with the exocyclic N2 amino group, with C(Me) · · · H(N2) and H(Me) · · · H(N2) distances of 2.74 and 2.34 Å, respectively. The other methyl group at the terminus of the carboxamide group is in close contact with hydrogen atoms on the strand 1 backbone, such as H(C1′) on the 3′ side of the intercalation site. The quinoline chromophore stacks on the strand 2 guanine base at the intercalation site, with almost perfect overlap of the six-membered rings. There is good overlap with the strand 2 guanine, partial with the strand 1 guanine, and none at all with either cytosine ring.

The model with the carboxamide side-chain in the major groove (Fig. 4), is of 3.1 kcal mol^{-1} higher energy than the minor groove one discussed above. Here, the side-chain protrudes out into the center of the groove and, thus, does not lie close to either hydrophobic backbone. There is a geometrically feasible hydrogen bond from the terminal positively charged nitrogen atom of the side-chain to O6 of the strand 1 guanine, with distance H(N)· · ·O6(G) of 1.90 Å. This model has good stacking of the chromophore with both intercalation-site guanines, with each six-membered ring of the quinoline overlapping the six-membered ring of a guanine. There is no overlap with either cytosine.

2-Phenylquinoline-8-carboxamide 5. A stereochemically plausible arrangement was obtained with the side-chain of **5** in the DNA minor groove (Table 4, model 3), lying close to the strand 2 backbone with two H · · · H contact distances of 2.20 and 2.28Å. The phenyl ring lies in the minor groove, where it is not stacked with any base but is aligned approximately parallel to the wall of the groove (Fig. 5). The closest contact between a hydrogen atom of the phenyl ring and a backbone H5′ atom is 2.37 Å. There is some chromophore stacking with the strand 1 guanine base and none at all with either cytosine or the strand 2 guanine.

The model (Table 5, model 4) with the side-chain in the major groove necessarily has the phenyl group in the same groove, with the molecule as a whole being held tightly in this position (Fig. 6). Any significant translational or rotational movement in the intercalation plane was found to result in severe steric clashes. The phenyl group protrudes out into the major groove at the optimal position for the molecule, whereas the carboxamide side-chain is in close contact with the hydrogen atoms attached to the 2′-position of the strand 2 guanosine sugar residue; the closest contact distances are 2.25 and 2.18 Å. It is notable that the two bases on this strand have been appreciably rolled open, by approximately 5–6°, during the energy refinement, to accommodate the side-chain. The quinoline chromophore has significant overlap with and is, thus, sandwiched between both bases of the other strand.

The net calculated binding energies of these two models, 3 and 4, are very similar (Table 4) with the slight superiority of the latter being possibly ascribable to greater quinoline-base pair stacking.

An alternative conformation was also examined for complexes of compound **5** with the carboxamide side-chain rotated by 180° about the C8-C17 bond, so as to result in the crystallographic conformation with the carbonyl oxygen atom O17 and the quinoline ring nitrogen atom N1 *cis* to each other. Because the modelled structure does not have a hydrogen atom attached to N1, there is no intramolecular 017 · · · N1 hydrogen bond and, thus, there is some 2–3 kcal mol^{-1} loss of energy compared with the *trans* conformers used for most of the modelling. This small energy difference has not been quantitated and, hence, is not reflected in the values in Table 4. The

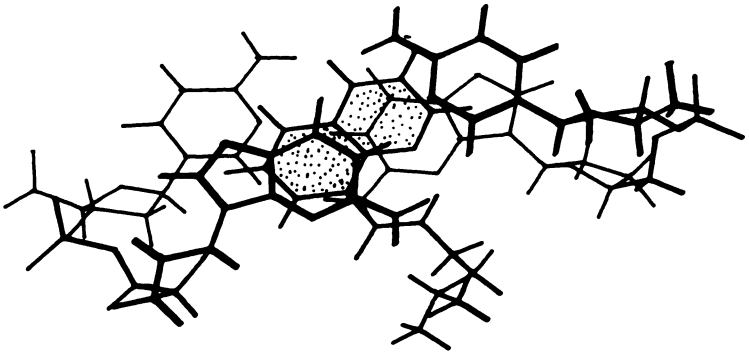

Fig. 3. View of the model for compound 4, looking onto the base pair plane. The quinoline chromophore is *shaded* and the view has clipped away all base pairs and DNA backbone except for those immediately at the intercalation site. This is designated the minor groove model, with the side-chain residing in this groove.

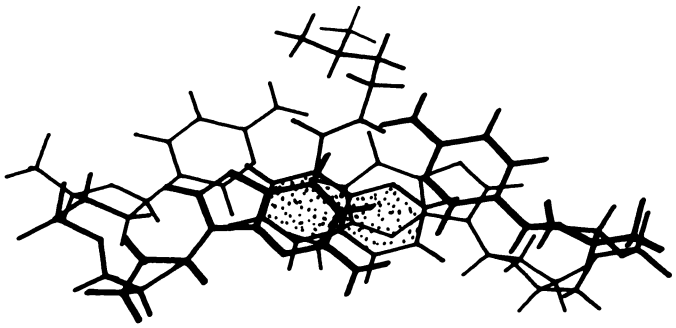

Fig. 4. The major groove intercalator model for 4.

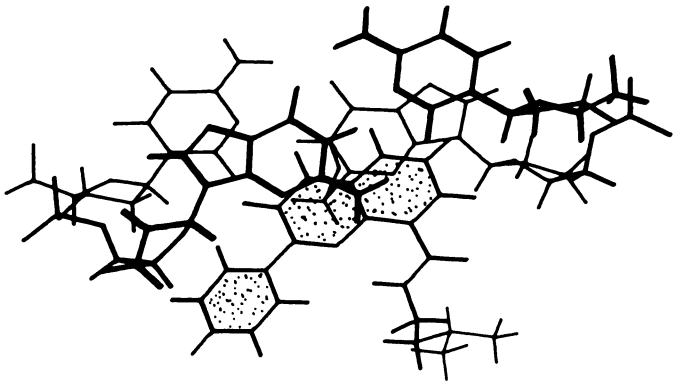

Fig. 5. The minor groove intercalation model for 5. Both phenyl and quinoline rings are *shaded*.

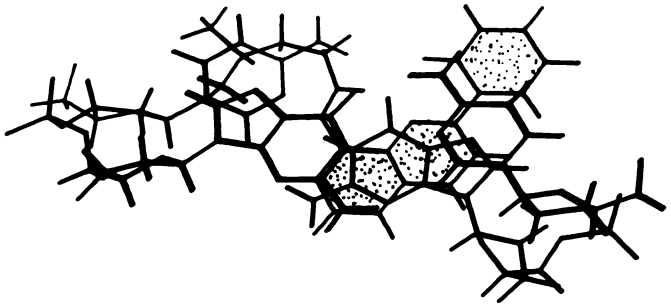

Fig. 6. The major groove intercalation model for 5.

cis conformation could only produce reasonable geometries for intercalation complexes with compounds 5 and 9.

The complex of 5 with the side-chain in the DNA minor groove (Table 4, model 5) has several of its methylene hydrogen atoms in close contact with the strand 2 backbone, with distances from them to H4′, H5′ of 2.32, 2.26, and 2.35Å (Fig. 7).

The phenyl ring of 5 is in the major groove, where it partially stacks on the strand 2 cytosine. These two planar rings are approximately coplanar. The twist of the base pair here is approximately 10°, which complements in sign and magnitude the dihedral angle of 11.7° for the phenyl ring with respect to the quinoline chromophore (Fig. 8). The base pair-quinoline stacking is restricted to the strand 1 guanine. This arrangement is of low energy, with the calculated energy of the drug itself being no higher than in the *trans* conformation. The torsion angel around the C8-C17 bond is −23.5°.

The only other plausible intercalation arrangement for the *cis* conformer of 5 is with both side-chain and phenyl group in the major groove. The former is very close to the strand 1 backbone of the DNA, with an H · · · H contact involving a terminal methyl group of the side-chain and a strand 1 cytosine N4 hydrogen atom (2.04 Å). There is also a close contact of 2.16 Å between a quinoline hydrogen atom and a cytosine deoxyribose H(C2′) atom of strand 2. There is minimal stacking of the chromophore in the intercalation site, with partial in-

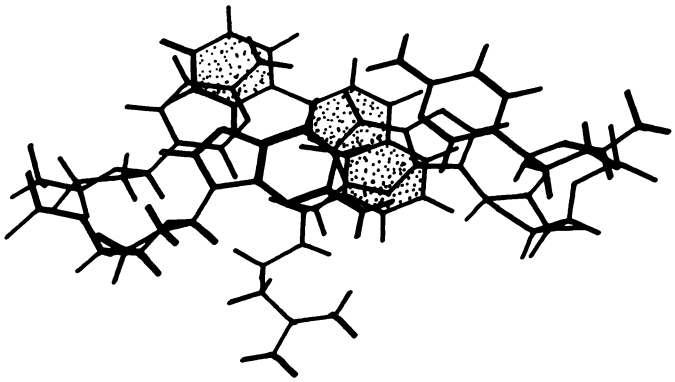

Fig. 7. The alternative, low energy minor groove model for 5.

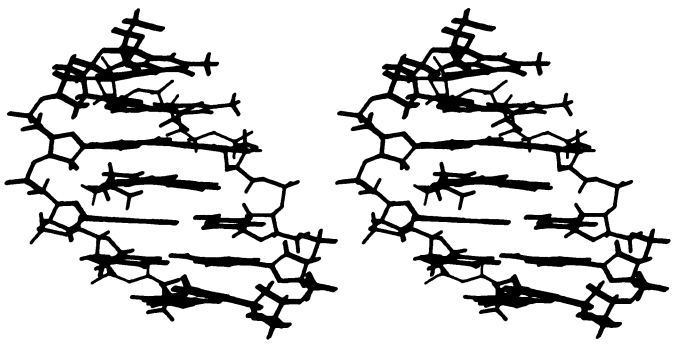

Fig. 8. A stereo view of the low energy model for 5, looking from the major groove direction.

volvement of the strand 2 cytosine. This arrangement (model 6) has the highest energy of any examined for **5**; it could not be diminished by rotational, translational, or torsional adjustments of the drug in the intercalation site because the drug-DNA fit was exceptionally tight.

3-Phenylquinoline-8-carboxamide 6. The clearly preferred orientation for this molecule with its side-chain in the minor groove of the DNA requires the phenyl substituent to be in the major groove, where it stacks effectively with the strand 2 cytosine base (Fig. 9). The bases on this strand are somewhat rolled open to accommodate the phenyl ring because it is not fully coplanar with either one. The quinoline chromophore stacks between the bases of strand 2, with most overlap being with the guanine. The carboxamide side-chain approaches closer to strand 1, although there are no close H · · · H distances of less than 2.62 Å. The alternative model (model 8) was found to have the phenyl group residing in the minor groove when the side-chain was in the major one (Fig. 10). The necessity to avoid steric clashes with the hydrogen atoms of the phenyl ring has forced the side-chain to be positioned centrally in the major groove and not to be in close contact with any backbone atoms. The phenyl ring is close to, but not in close contact with, the walls of the minor groove. The quinoline chromophore has partial overlap with the strand 1 guanine base, minimal with the other guanine, and none with the two cytosines at the intercalation site. The calculated binding energy for this model is significantly less favored than the minor groove side-chain one (model 7).

4-Phenylquinoline-8-carboxamide 7. The low energy position for this compound with its side-chain in the minor groove has the phenyl ring in the major groove (model 9; Fig. 11). The hydrogen atoms of the phenyl ring adjacent to the phenyl-quinoline bond are in close contact with base hydrogen atoms of strand 2. Thus, there is a H(Phe) · · · HN4 (cytosine) distance of 2.15 Å and a H(Phe)· · · · HC8 (guanine) distance of 2.35 Å. In contrast, the side-chain does not come close to either backbone strand in the minor groove, with closest H · · · H distances being no less than 2.45–2.50 Å from H4′,H5′ backbone atoms to the methylene hydrogen atoms in the chain. The chromophore **7** is stacked exclusively between the bases of strand 2.

The alternative model, model 10, with the phenyl group in the minor groove, has the side-chain in the major groove, close to the strand 1 backbone so that there are a number of close interatomic contacts (Fig. 12). In particular, a phosphate oxygen atom of the intercalation site is close to a terminal methyl group of the side-chain, with distances O(P) · · · H(Me) of 2.65 and 2.79 Å. Stacking of the quinoline ring system with base pairs is slight, with only the guanine of strand 2 being involved. The binding energy for this arrangement is slightly less than for model 9.

5-Phenylquinoline-8-carboxamide 8. The low energy arrangement (model 11) with the side-chain in the minor groove (Fig. 13) has it positioned in the center of the groove, with the sole close contacts being between a methylene hydrogen atom and the exocyclic amino group of the strand 2 guanine at the intercalation site (the H(Me) · · · H(N2) distance is 2.17 Å). The phenyl group sits in the major groove without there being any H · · · H close contacts less than 2.35 Å. The quinoline chromophore stacks with the strand 2 guanine and, partially, with the strand 1 guanine; there is no overlap with either cytosine. The low energy model (Table 5, model 12) with the side-chain of **8** in the major groove has a terminal methyl group hydrogen close to the O6 atom of the strand 1 guanine base

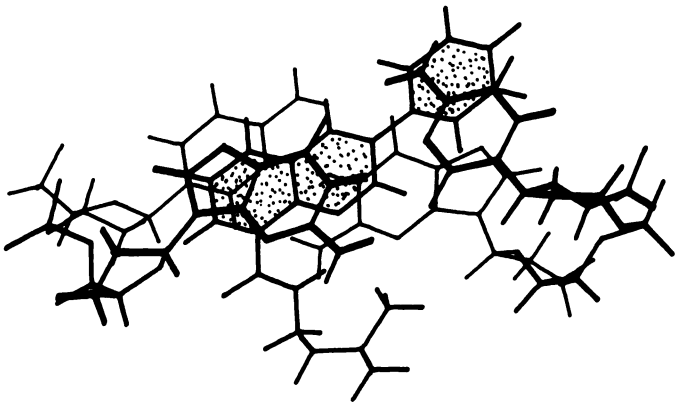

Fig. 9. Minor groove intercalation model for **6**.

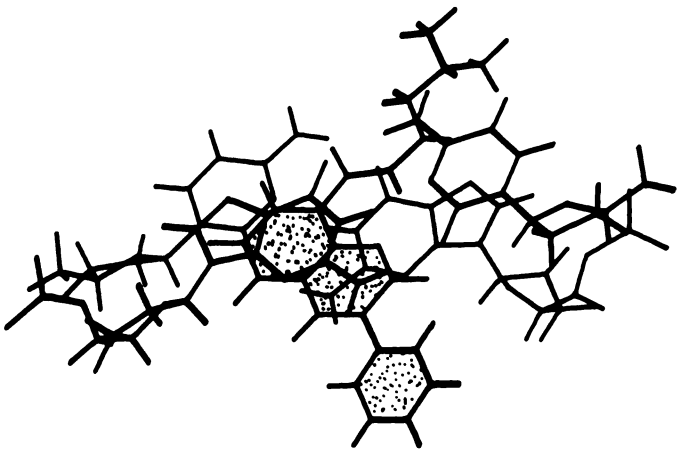

Fig. 10. Major groove intercalation model for **6**.

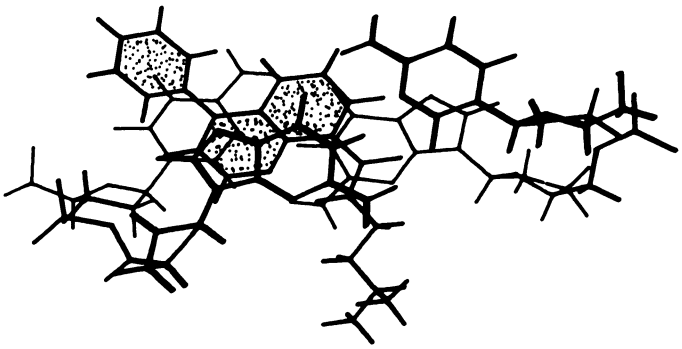

Fig. 11. Minor groove intercalation model for **7**.

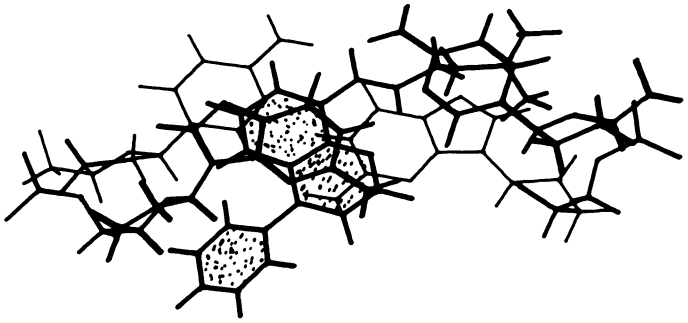

Fig. 12. Major groove intercalation model for **7**.

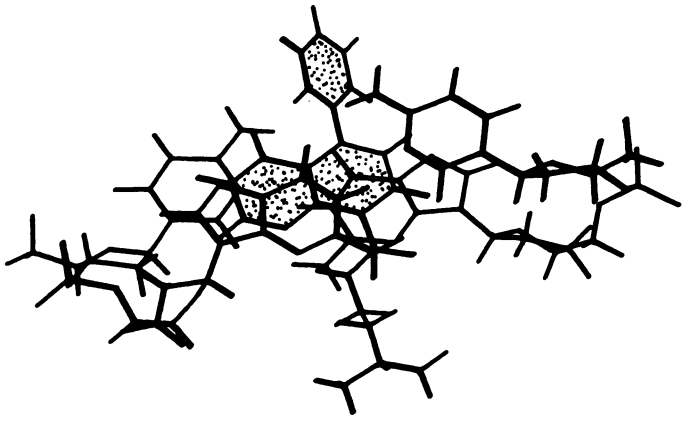

Fig. 13. Minor groove intercalation model for 8.

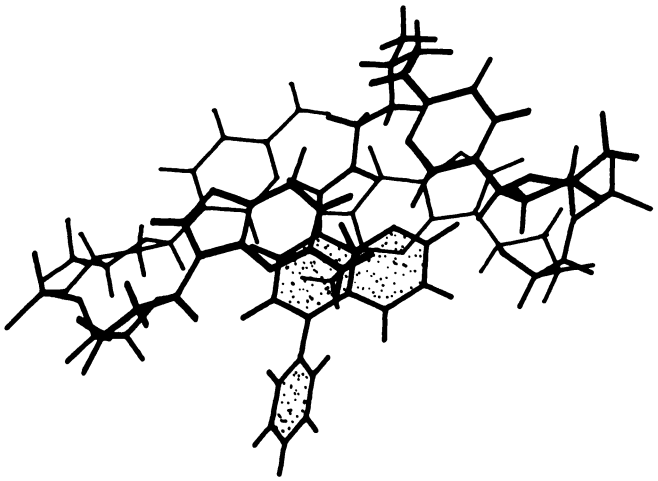

Fig. 14. Major groove intercalation model for 8.

(the H · · · O6 distance is 2.75 Å). The phenyl ring substituent lies in the minor groove and is oriented parallel to the direction of the phosphodiester backbone of strand 2 such that the flat surface of the ring lies close to the wall of the groove (Fig. 14). There are several close contacts between the phenyl atoms and backbone atoms, notably between the H4′ on the 3′ side of the intercalation site and a phenyl carbon atom (2.68 Å). The quinoline chromophore is very minimally stacked on the strand 2 guanine and not at all on the other bases. The relative binding energies of models 11 and 12 favor the former; as for compound **7**, the difference between major and minor groove models is less than for other compounds in the series.

6-Phenylquinoline-8-carboxamide 9. The minor groove model (model 13; Fig. 15) for this compound has the largest computed binding energy for any model in the series. The carboxamide side-chain in this model is in close contact with the strand 2 backbone (Fig. 16). The second methylene (C21) has one of its hydrogen atoms close to the C5′ hydrogen atom at the 3′ end of the strand 2 guanosine with an H · · · H distance of 2.16 Å. One of the terminal methyl groups comes in close contact with the H4′ and H5′ atoms of the strand 2 guanosine, with H · · · H separations of 2.24 and 2.23 Å. The phenyl ring substituent lies to one side of the major groove and stacks effectively with the strand 1 cytosine. The phenyl ring and this cytosine are approximately parallel, as are the quinoline chromophore and the strand 2 guanine (which are well stacked together). Thus, the twist angle of 24.5° between phenyl

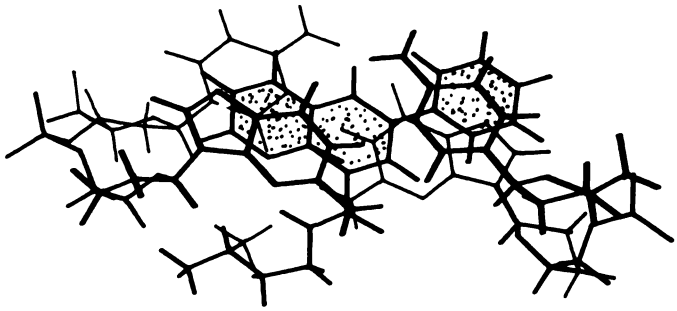

Fig. 15. Minor groove intercalation model for 9.

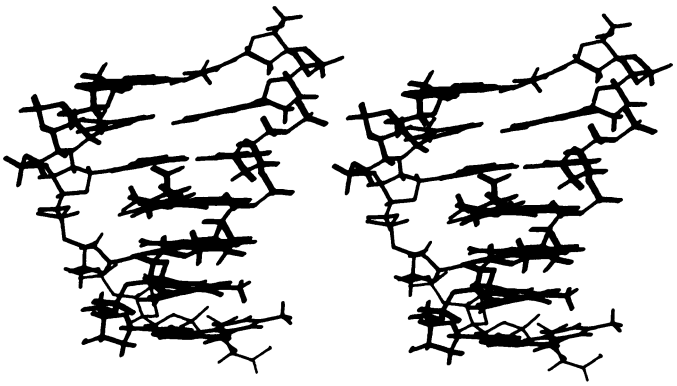

Fig. 16. Stereo view of the minor groove model for 9, looking into the minor groove of the DNA.

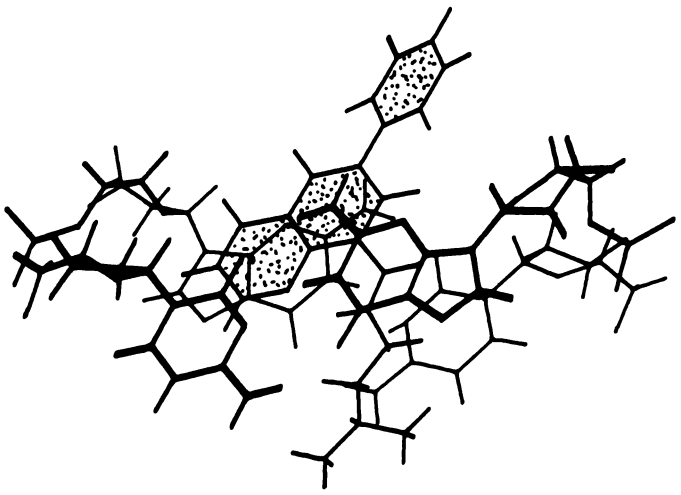

Fig. 17. Major groove intercalation model for 9.

group and quinoline is close to the twist angle subtended by these two bases.

The alternative model with the side-chain in the major groove is more than 11 kcal mol^{-1} higher in energy (Fig. 17). Neither the side-chain nor the minor groove phenyl group are in close contact with any atoms of the DNA; chromophore-base overlap is confined to the strand 2 guanine. As with compound **5**, an alternative conformation for the carboxamide side-chain was found to be possible, and two intercalation models resulted from the graphics modelling and energy refinement. One, model 15, has both side-chain and phenyl group positioned in the DNA minor groove. The side-chain is close to strand 1, with H · · · H contacts involving the methylene atoms and H4′,H5′ at the "intercalation site" and H · · · H distances of 2.20 and

TABLE 6

Selected carboxamide torsion angles (°) in the DNA complexes after energy refinement

The atoms defining the torsion angles are C7-C8-C17-N8 and C3-C2-C11-C16, except for models 5, 6, 15, and 16, where C9-C8-C17-O17 was used.

Model Number	C8-C17 Bond	C2-C11
1	−0.3	
2	21.5	
3	11.8	31.3
4	−38.5	14.2
5	−23.5	11.7
6	28.0	29.6
7	−23.1	31.9
8	8.7	18.0
9	−8.9	39.8
10	−28.0	43.6
11	7.1	35.9
12	−10.1	48.8
13	−18.7	24.5
14	4.9	34.1
15	33.4	31.9
16	−14.8	41.7

TABLE 7

Experimental physicochemical and biological data for compounds 4–9 (from Ref. 10), compared with computed binding energies

Compound	Unwinding Angle[a]	log K^b	IC_{50}[c]	P388 ILS[d]	ΔE^e	ΔG^f
			nM		kcal mol^{-1}	kcal mol^{-1}
4	0°	5.15	725000	NA	−15.9	−12.7
5	14°	5.95	1300	91	−21.6	−14.7
6	20°	5.69	2600	27	−20.2	−14.0
7	0°	4.75	14700	NA	−19.4	−10.8
8	0°	4.76	13700	NA	−18.3	−11.8
9	20°	6.04	910	29	−25.7	−14.9

[a] Relative to a value of 26° determined for ethidium.
[b] Equilibrium binding constants determined by means of the ethidium displacement method. Mean of values found for poly [d(AT)] and poly [d(GC)].
[c] For L1210 leukemia cells in culture. This is the drug concentration (nM) that reduces cell growth to 50% of controls after 70 hr.
[d] Percentage increase in lifespan of treated animals with intraperitoneally injected P388 leukaemia cells. NA indicates inactive compounds.
[e] Binding energies, in kcal mol^{-1} for the "best" binding mode, from Table 5.
[f] Free energies of binding, in kcal mol^{-1}, calculated from the K values using $\Delta G = -RT \cdot \ln K$.

2.35 Å. The phenyl ring is pushed out into the groove and does not come close to any DNA atoms. There is no chromophore-base overlap at all. The alternative model with both groups in the major groove has the lowest binding energy of any in the series. There are no close contacts between any of the DNA atoms and either the phenyl ring or the side-chain, which protrude into the groove. There is some stacking of the chromophore of **9** with the strand 1 guanine base.

Discussion

Crystal structure analysis of the 2-phenylquinoline-8-carboxamide **5** has shown that, even under the relatively mild crystallization conditions used, both nitrogen atom sites are protonated in the crystalline state, even though one of them, the quinoline ring nitrogen atom, is weakly basic with a pK_a of around 3 (10) and is, thus, unprotonated in solution at physiological pH. Thus, the intramolecular hydrogen bonding between this nitrogen atom and the carboxamide side-chain would be expected to be between the nitrogen as acceptor and the amide side-chain nitrogen as donor; this situation was observed in the crystal structures of the two analogous free-base acridine carboxamides (14). The barrier to rotation about the C8-C17 bond, by analogy with that calculated for these acridine carboxamides, is low, with the hydrogen-bonded conformation being preferred by about 2.5 kcal mol^{-1} over the 180° rotamer (which represents the crystallographic conformation, albeit of the protonated form, found in the present study). The low energy domains for rotation about this bond and about the C2-C11 bond (linking quinoline to phenyl groups) have emerged as being relatively broad from the molecular mechanics calculations (Table 6).

The molecular modelling of intercalative-type interactions for compounds **4–9** in the CpG site in the d(TACGTA) duplex has indicated that there are marked quantitative and qualitative differences between the complexes for each compound, the most stable models having their side-chain lying in the DNA minor groove. The experimental data on DNA affinities for the series (10) enables detailed comparisons between theory and experiment to be made. The data of Table 7 show that compounds **4**, **7**, and **8** are poor intercalators. The other three compounds have significantly higher association constants, in the order **9** > **6** > **5**, as well as being normal intercalators, although this order is not given by the measured unwinding angles.

The simulated intercalative bindings of **4**, **7**, and **8** are all characterized by having only their quinoline chromophore stacked between base pairs, in contrast to the best (minor groove) models for **5**, **6**, and **9**, which have their phenyl groups involved in stacking as well. This qualitative difference was earlier predicted (10) on the basis of an examination of CPK models. The position of attachment of the phenyl ring is, therefore, the major determinant of intercalative ability, with effective binding that results in experimentally detected intercalation requiring stacking interactions involving more than the two aromatic rings of the quinoline. Compounds **4**, **7**, and **8** have been treated as pseudo-intercalators in the absence of any plausible structural model for nonintercalative binding. Drug-base pair stacking interactions do not by themselves provide sole discrimination between the different models in Table 5. Crucial roles are played by differences in close intermolecular contacts involving side-chain, and to a lesser extent phenyl group, atoms, with the relatively tight fit of the side-chain in the DNA minor groove being between the hydrophobic walls of the two strands. These walls are to a large extent lined with hydrogen atoms from the sugar-phosphate backbones, and there are numerous attractive close contacts between them and atoms of compounds **4** and **9**, as detailed above. In several instances, the close contacts are indicative of possible hydrogen bonding. The force field used here does not have an explicit hydrogen-bonding component but instead considers such an interaction to be an electrostatic one. The superiority of model 13 for compound **9** over other models is probably largely due to its very effective phenyl group stacking. By contrast, the major groove model 16 for **9**, even though it has some quinoline-guanine stacking, has no close contacts at all between side-chain and phenyl ring and the DNA groove atoms. In the case of model 6 for compound **5**, the relative disposition of the side-chain and phenyl groups produces too bulky an arrangement for comfortable positioning in even the major groove and, thus, this model has some close repulsive contacts with distances less than van der Waals separation.

The binding energies calculated here do not directly take account of any differences in solvation between different complexes or between drug-bound and drug-free DNA (23). It has not been feasible with our computer resources to consider modelling explicit solvent structures for these complexes. Thus, these ΔE values cannot be formally compared with experimentally derived free energies (Table 7). However, the fact that the present study has used the same (CpG) intercalation site for all the models examined provides a test for any major solvation differences between the models. It has been pointed out that ΔE comparisons of ligand binding to different sequences is more problematic (23), and, moreover, for these drugs there is no evidence of marked sequence preferences. We would, thus, expect analogous calculations on AT intercalator sites to produce a similar ranking order of ΔE values. The numerical values of ΔE and ΔG correspond moderately well, suggesting that the scaling of the relatively large electrostatic component of the force field by a $4r_{ij}$ term is a satisfactory procedure. It is notable that the ranking order of the calculated ΔE values, with that for compound **9** being the largest, is in overall good agreement with the order of ΔG values. The differences between models, up to nearly 10 kcal mol^{-1}, for ΔE values is considerably greater than for the ΔG ones, suggesting that there are some differences in desolvation between the models but that they are not major ones. It should, nevertheless, be realized that the measurements of DNA affinities by ethidium displacement may not provide strict comparison with equilibrium binding constants obtained by analysis of binding curves. The good correlations between observed and calculated energies and *in vitro* cytotoxic activity (Table 7) lends further support to the hypothesis that the extent of intercalative ability is a major factor in the cytoxicity shown by this series of DNA-binding compounds. The poorest DNA binders of the series (compounds **4**, **7**, and **8**) show very low potency, which extends to their lack of *in vivo* activity (10), whereas the other three intercalating compounds are all active (to varying extents) against the P388 leukaemia.

In conclusion, this study has provided a quantitative molecular basis for the DNA-binding behavior and biological activity of a series of phenyl-substituted quinoline-8-carboxamides. Molecular modelling has correctly indicated the overall order of DNA affinity in the series, which also suggests that the intercalation model used here has relevance for the conformation of the binding site in solution, although detailed confirmation must await the results of X-ray or NMR analyses.

References

1. Waring, M. J. DNA-binding characteristics of acridinylmethane-sulphonanilide drugs: comparison with antitumour properties. *Eur. J. Cancer* **12**:995–1001 (1976).
2. Baguley, B. C., W. A. Denny, G. J. Atwell, and B. F. Cain. Potential antitumor agents. 34. Quantitative relationships between DNA binding and molecular structure for 9-anilinoacridines substituted in the anilino ring. *J. Med. Chem.* **24**:170–177 (1981).
3. Baguley, B. C., W. A. Denny, G. J. Atwell, and B. F. Cain. Potential antitumor agents. 35. Quantitative relationships between antitumor (L1210) potency and DNA binding for 4′-(9-Acridinylamino)methanesulfon-*m*-anisidide analogues. *J. Med. Chem.* **24**:520–525 (1981).
4. Wilson, W. R., B. C. Baguley, L. P. G. Wakelin, and M. J. Waring. Interaction of the antitumor drug 4′-(9-acridinylamino)methane-sulfon-*m*-anisidide and related acridines with nucleic acids. *Mol. Pharmacol.* **20**:404–414 (1981).
5. Neidle, S., G. D. Webster, B. C. Baguley, and W. A. Denny. The crystal structure of 1-methylamsacrine hydrochloride; relationships to DNA-binding ability and anti-tumour activity. *Biochem. Pharmacol.* **35**:3915–3921 (1986).
6. Atwell, G. J., F. Cain, B. C. Baguley, G. J. Finlay, and W. A. Denny. Potential antitumor agents. 43. Synthesis and biological activity of dibasic 9-aminoacridine-4-carboxamides, a new class of antitumor agent. *J. Med. Chem.* **27**:1481–1485 (1984).
7. Rewcastle, G. W., G. J. Atwell, D. Chambers, B. C. Baguley, and W. A. Denny. Potential antitumor agents. 46. Structure-activity relationships for acridine monosubstituted derivatives of the antitumor agent *N*-[2-(dimethylamino)ethyl]-9-aminoacridine-4-carboxamide. *J. Med. Chem.* **29**:472–477 (1986).
8. Atwell, G. J., G. W. Rewcastle, B. C. Baguley, and W. A. Denny. Potential antitumor agents. 50. *In vivo* solid-tumor activity of derivatives of *N*-[2-(dimethylamino)ethyl]acridine-4-carboxamide. *J. Med. Chem.* **30**:664–669 (1987).
9. Denny, W. A., I. A. G. Roos, and L. P. G. Wakelin. Interrelations between anti-tumour activity, DNA breakage, and DNA binding kinetics for 9-aminoacridinecarboxamide anti-tumour agents. *Anti-Cancer Drug Design* **1**:141–147 (1986).
10. Atwell, G. J., C. D. Bos, B. C. Baguley, and W. A. Denny. Potential antitumor agents. 56. "Minimal" DNA-intercalating ligands as antitumor drugs: phenylquinoline-8-carboxamides. *J. Med. Chem.* **31**:1048–1052 (1988).
11. Main, P., S. J. Fiske, S. E. Hull, L. Lessinger, G. Germain, J.-P. Declercq, and M. M. Woolfson. *MULTAN82: A System of Computer Programs for the Automatic Solution of Crystal Structures from X-Ray Diffraction Data.* Universities of York, England, and Louvain, Belgium. (1982).
12. Frenz, B. A., and Associates. Inc. *SDP: Structure Determination Package.* College Station, TX and Enraf-Nonius, Delft, The Netherlands (1983).
13. Walker, N. L., and D. I. Stuart. An empirical method for correcting diffractometer data for absorption effects. *Acta Crystallogr.* **A39**:158–166 (1983).
14. Hudson, B. D., R. Kuroda, W. A. Denny, and S. Neidle. Crystallographic and molecular mechanics calculations on the anti-tumor drugs *N*-[(2-dimethylamino)ethyl]- and *N*-[(2-dimethyl-amino)butyl]-9-aminoacridine-4-carboxamides and their dications: implications for models of DNA-binding. *J. Biomol. Struct. Dyn.* **5**:145–158 (1987).
15. *GEMINI: Graphics Emulation of Molecules by INteractive Instructions.* The Institute of Cancer Research, Sutton, Surrey, UK (1989).
16. Neidle, S., L. H. Pearl, P. Herzyk, and H. M. Berman. A molecular model for proflavine-DNA intercalation. *Nucleic Acids Res.* **16**:8999–9016 (1988).
17. Shieh, H.-S., H. M. Berman, M. Dabrow, and S. Neidle. The structure of a drug-deoxydinucleoside phosphate complex: generalised conformational behaviour of intercalation complexes with RNA and DNA fragments. *Nucleic Acids Res.* **8**:85–87 (1980).
18. Weiner, S. J., P. A. Kollman, D. T. Nguyen, and D. A. Case. An all atom force field for simulations of proteins and nucleic acids. *J. Comput. Chem.* **7**:230–252 (1986).
19. Abraham, Z. H. L., M. Agbandje, S. Neidle, and R. M. Acheson. Experimental DNA binding and computer modelling studies on an analogue of the antitumour drug amsacrine. *J. Biomol. Structure Dyn.* **6**:471–488 (1988).
20. Whitlow, M., and M. M. Teeter. An empirical examination of potential energy minimisation using the well-determined structure of the protein crambin. *J. Am. Chem. Soc.* **108**:7163–7172 (1986).
21. Haneef, I. Ph.D. Thesis, University of London (1985).
22. Gdaniec, M., M. Jaskolski, and Z. Kosturkiewicz. Quinoline-2-carboxamide. *Acta Crystallogr.* **B33**:3558–3561 (1977).
23. Lybrand, T., and P. Kollman. Molecular mechanical calculations on the interaction of ethidium cation with double-helical DNA. *Biopolymers* **24**:1863–1879 (1985).

Send reprint requests to: Dr. S. Neidle, CRC Biomolecular Structure Unit, Institute of Cancer Research, Cotswold Road, Sutton, Survey SM2 5NG, United Kingdom.